บทที่ 6
สรุปผลผลิตงานวิจัย

สรุปรายชื่อและรายละเอียดผลผลิตงานวิจัยที่ผลิตได้

6.1 ชื่อบทความวิจัย “Effect of Oxidation Temperature on the Properties of CuO Thin Films Prepared by Thermal Oxidation of Sputtered Cu Thin Films” ตีพิมพ์ใน Advanced Materials Research vol. 1098, 2015, pp. 6-11. โดยมีรายละเอียดดังนี้คือ

ABSTRACT

CuO thin films were obtained through thermal oxidation of dc magnetron sputtered metallic Cu films on glass substrates. Thermal oxidation process was performed in air at temperature ranging 300-500^{O}C. From XRD patterns, CuO single phase of monoclinic structure was formed at oxidation temperature beyond 450^{O}C whereas amorphous phase with very small grains was obtained at oxidation temperature below 450^{O}C. The positive sign of the Hall coefficient confirmed the p-type conductivity in all studied films. From transmission spectra, direct band gap value is varied between 2.17 and 2.83eV. From the transient photoconductivity measurements, persistent photoconductivity (PPC) behavior was observed. The decay current data were better fitted with the multiple exponential functions resulting into five slow decay times. Density of trap states corresponding to its decay time was also evaluated from the decay current data.

Keywords: p-CuO/n-CdS heterojunction, I-V characteristics, C-V characteristics

INTRODUCTION

Oxides of copper are well-known to show p-type conductivity and have many advantages for catalysts and solar energy conversion application. Non-toxic, economic, abundant availability and relatively simple formation of oxide makes copper oxide as an interesting material [1]. Two common forms of copper oxide are cuprous oxide (Cu_2O) and cupric oxide (CuO). A meta-stable copper oxide, Cu_4O_3, which is an intermediate compound between the previous two, has also reported [2]. Cu_2O and CuO belong to cubic and monoclinic structures with band gap of 2.1-2.6 eV and1.9-2.1eV, respectively. The growth of high quality p-type CuO thin films is essential for fabricating p-n junction-based oxide devices, such as solar cells, light emitting diodes and transistors. The optical transmittance and electrical resistivity of the films are two critical parameters in evaluating the performance of

photovoltaic cells and electrochromic devices. In this paper, CuO thin films were obtained through thermal oxidation of dc magnetron sputtered metallic Cu films on glass substrates. The physical properties of the films were studied in order to find the possibility to use them in p-n junction low cost thin film solar cells.

EXPERIMENTAL

Copper thin films were grown on glass substrates by using dc magnetron sputtering from a home-made circular planar magnetron sputtering system. A circular planar magnetron of 60 mm diameter was used as the magnetron cathode. The magnetron target assembly was mounted on the top plate of the sputter chamber such that the sputtering could be done by sputtering down configuration. A continuously variable dc power supply of 630 V and 2.6 A was used a power source for sputtering. A 60 mm diameter and 3 mm thick pure copper (99.99%) used as sputter target. Pure argon was used as sputter gas. The flow rate of argon was controlled by AALBORG mass flow controller. Before deposition of each batch, the target was sputtered in pure argon atmosphere for 5 min to remove oxide layer if any on the surface of target. The sputtering conditions maintained during the growth copper films are given in Table 1. The as-deposited copper thin films were oxidized in tubular furnace at temperature ranging from 300-500 ^{o}C in air for 60 min. The crystal structure of these films was checked by X-ray diffraction technique with a Brucker D 8 diffractometer using CuK_{α} radiation. Surface morphology was examined by JEOL model JSM-6400 scanning electron microscope. Optical transmission measurements were performed with UV-VIS double beam spectrophotometer in the wavelength range of 220-1,000 nm. The band gap (E_g) of the transparent films was determined by using the equation $(\alpha h\nu)^2 = A(h\nu - E_g)$ where α is the absorption coefficient, A is a constant and $h\nu$ is the photon energy. Electrical properties of the films were evaluated by Hall effect and resistivity measurements in the van der Pauw configuration at room temperature.

Table 1 List of some conditions for preparing CuO thin films

Conditions	Parameters	Values
Sputtering	Target	Cu
	Argon flow rate (sccm)	15
	Target to substrate distance (cm)	10
	Bias voltage (V)	370
	Current (mA)	80
	Substrate temperature (^{o}C)	25
	Working pressure (torr)	$3.6x10^{-3}$
	Sputtering time (min)	6
Oxidized in air	Temperature (^{o}C)	300-500
	Time (min)	60

RESULTS AND DISCUSSION

Fig. 1 shows XRD patterns of CuO films as a function of oxidation temperature. XRD patterns of the films oxidized at temperature below 450^{O}C show amorphous characteristics. In contrast, the XRD spectrum of the films oxidized at 500^{O}C shows the well-resolved two diffraction peaks. These peaks correspond to the reflection of (-111) and (111) planes of standard JCPDS data card of CuO (JCPDS No. 80-1268). The crystallite size was calculated using Scherrer's formula, neglecting peak broadening due to residual stresses in the films, $L= 0.9\lambda/(\beta\cos\theta)$ where β is the broadening of diffraction line measured at half its maximum intensity in radian and λ is the wavelength of X-rays (0.1540 nm). The calculated value of L is about 15 nm. SEM images of CuO films obtained from oxidation temperature during 300-500^{O}C were shown in Fig. 2. When the films were oxidized below 350^{O}C, the morphology does not change much and shows better uniformity in free surface. However, oxidation temperatures higher than 350^{O}C, small pores over the films were observed.

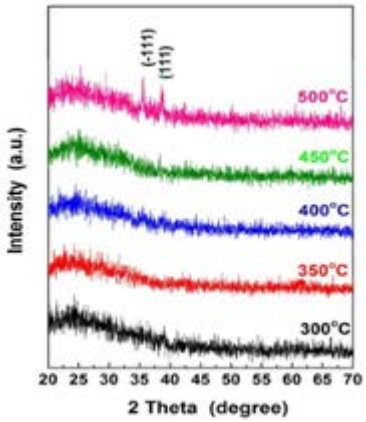

Fig. 1 XRD patterns of CuO films as a function of oxidation temperature.

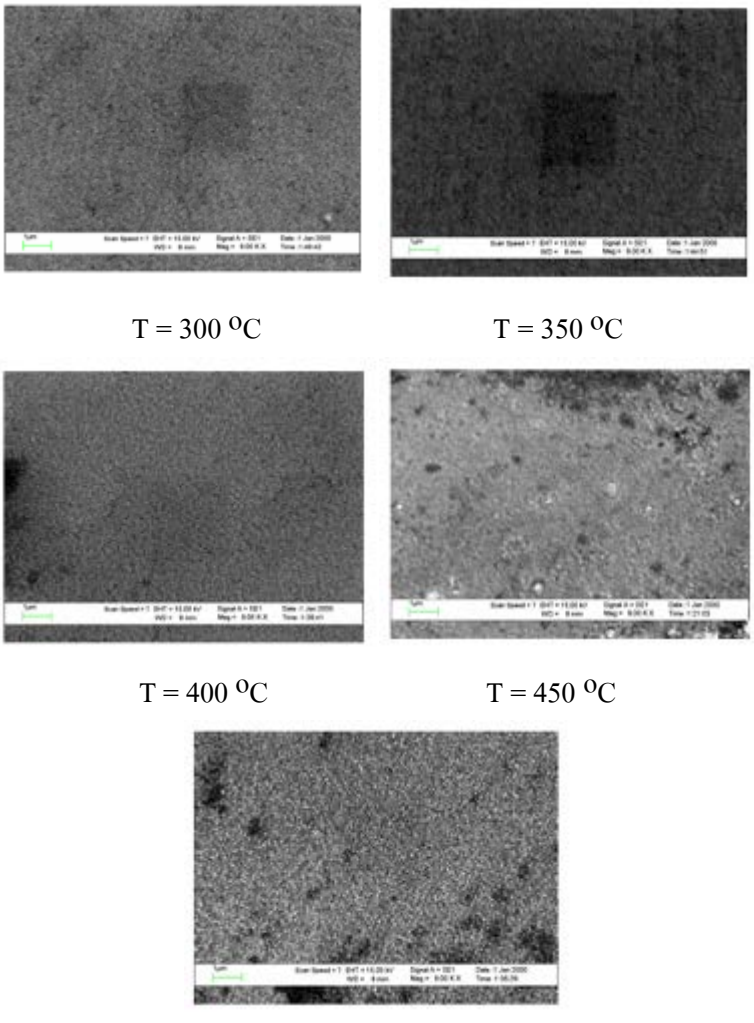

Fig. 2 SEM images of CuO films obtained from oxidation temperature between 300-500°C.

Fig. 3 shows transmittance spectra of CuO films obtained from oxidation temperature during 300-500^{o}C. From the transmittance spectra we have also calculated band gap of films with different oxidation temperatures. The absorption coefficient (α) is calculated using the equation $\alpha = (1/d)\ln(1/T)$ where T is transmittance and d is film thickness. The absorption coefficient (α) and the incident photon energy ($h\nu$) related by $(\alpha h\nu)^2=A(h\nu-E_g)$ where A and E_g are constant and band gap values, respectively. The E_g can be determined by extrapolation of the linear portion of the curve to the photon energy axis. Fig. 4 shows the curve of $(\alpha h\nu)^2$ vs. photon energy ($h\nu$) of the films obtained from oxidation temperature at 500^{o}C. Two allowed direct transition band gap were obviously observed. The smaller band gap value (E_{g1}) should correspond to the major CuO phase. The bigger band gap (E_{g2}) is possibly attributed to the parasitic phase of Cu_2O which cannot be observed by XRD due to too small amount of Cu_2O content in the bulk of films. The variation of E_{g1} and E_{g2} was shown in Fig. 5. The E_{g1} decreases from 2.41 to 2.17 eV with oxidation temperature increases from 300 to 400^{o}C and then increases to 2.19 eV when oxidation temperature further increases to 500^{o}C. The similar behavior is also observed in E_{g2}. These results indicate that E_{g1} and E_{g2} are sensitive to the oxidation temperature.

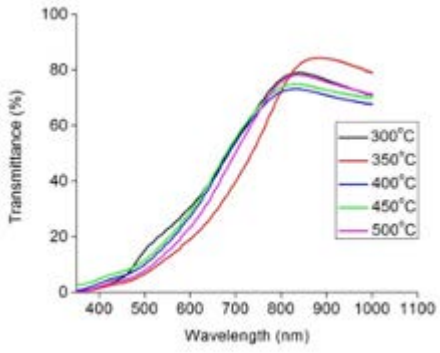

Fig. 3 Transmittance of CuO films obtained from oxidation temperature between 300-500 ^{o}C.

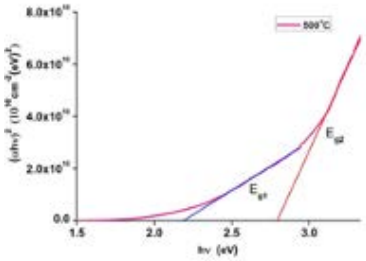

Fig. 4 $(\alpha h\nu)^2$ vs. $h\nu$ plot of CuO films obtained from oxidation temperature at 500 ^{o}C.

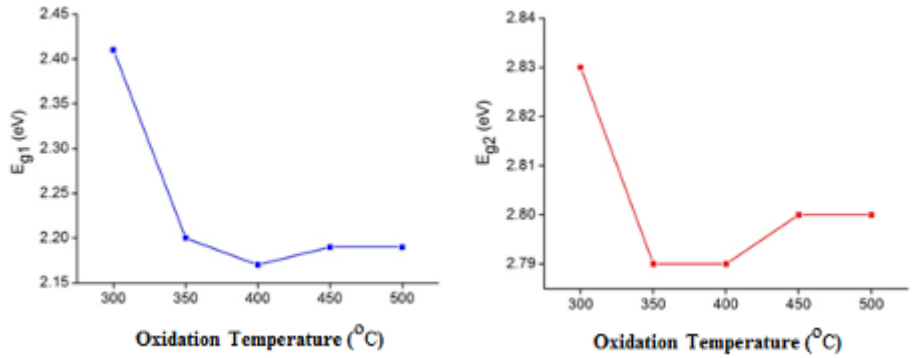

Fig. 5 Variation of band gap of CuO films as a function of oxidation temperature.

Electrical properties of the films were evaluated by Hall effect and resistivity measurements in the van der Pauw configuration. We found that all studied films are exhibited p-type conductivity. Variations of the resistivity, carrier concentration and mobility against oxidizing temperature are shown in Fig. 6. Carrier concentration (n) is derived from the relation $n=1/eR_H$ where R_H is the Hall coefficient and e is the absolute value of the electron charge. The carrier mobility (μ) is determined using the relation $1/ne\rho$ where ρ is resistivity. Resistivity of the films increases from $5.01\text{x}10^{2}$ to attain maximum at $7.50\text{x}10^{3}\Omega$.cm with oxidation temperature increasing from 300 to 400^{o}C, and decreases to $1.88\text{x}10^{3}\ \Omega$.cm when the oxidation temperature further increase to 500^{o}C. The mobility initially decreases with an increase in oxidation temperature up to 400^{o}C and then increases with an increase in oxidation temperature. The variation of carrier concentration shows the similar behavior to mobility. These results indicate that the resistivity, carrier concentration and mobility of the films are sensitive to the oxidation temperature.

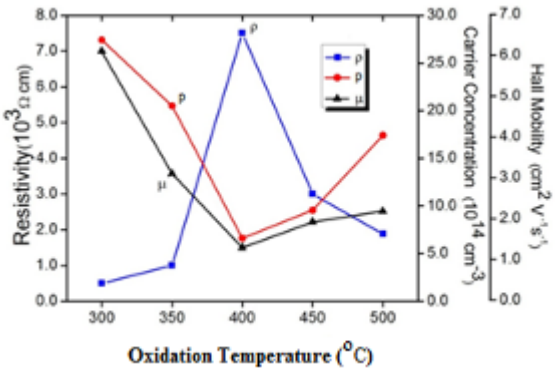

Fig. 6 Variations of the resistivity, carrier concentration and mobility against oxidation temperature.

The photocurrent response of the films oxidized at 500^{O}C was measured by two probe method using halogen lamp as a light source. Two silver electrodes with area 0.05 cm^{2} was made on the sample surface. The photocurrent response of the films oxidized at 500^{O}C was shown in Fig. 7. The sample was connected to the experimental setup and maintained in darkness under a constant applied bias of 6 V to stabilize the current. After the stabilization period, the current was recorded in the following sequences: 30 s in darkness, 400 s under illumination and, finally, 400 s in the darkness. Under illumination, the current increases immediately because a lot of carriers were exited by light illumination. After the illumination period, the persistent photoconductivity (PPC) effect of the films oxidized at 500^{O}C occurred in darkness. The decay of PPC in Fig. 7 can be described by multiple exponential functions [3,4] as

$$I = I_{dark} + (I_0 - I_{dark}) \sum_i \exp(-\frac{t}{\tau_i})$$

where I_{dark} is the current measured in darkness, I_0 is the PPC buildup level near the moment of light excitation being removed, τ is the PPC decay time constant. The normalized decay current in darkness as shown in Fig. 8, which follows the illumination period, indicates the persistent of charge carrier traps in the films [5]. In Fig. 8 the dash line is the measured data and the solid line is the least squares fit data by the multiple exponential functions as described above. According to the function of fitting curve in Fig. 8 we calculated that the five τ values are 120.77, 208.33, 414.94, 884.96 and 1504.95 s. Method for calculating the trap densities corresponding to the PPC decay constant was reported in the literatures [6-8]. The corresponding trap densities are 1.38x10^{11}, 1.03x10^{11}, 7.90x10^{10}, 6.70x10^{10} and 5.89x10^{10} cm^{-2}.

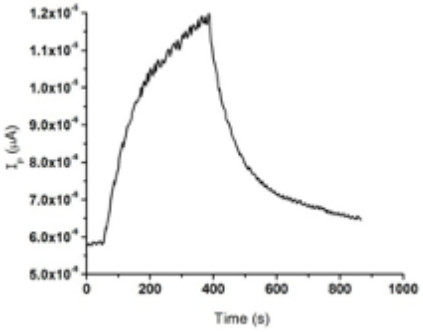

Fig. 7 Photocurrent response of CuO films obtained from oxidation temperature at 500^{O}C.

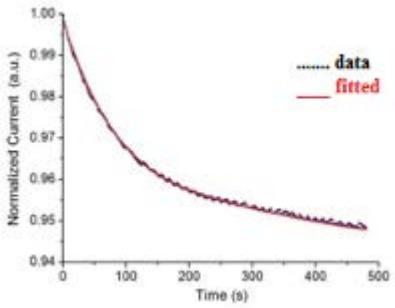

Fig. 8 Normalized decay time of CuO films obtained from oxidation temperature at 500^{O}C.

SUMMARY

CuO thin films were obtained through oxidation of metallic Cu films deposited on glass substrates by dc magnetron sputtering method. It is shown that the CuO single phase of monoclinic structure was formed at oxidation temperature beyond 450^{o}C where amorphous phase with very small grains, confirmed by SEM images, was obtained at oxidation temperature below 450^{o}C. All studied films are p-type semiconductors with band gap of 2.17-2.83 eV. The photocurrent response of films oxidized at 500^{o}C was measured by two probe using halogen lamp as a light source. The decay current data were better fitted with the multiple exponential functions. Five slow decay times and five trap densities values are 120.77, 208.33, 414.94, 884.96, 1504.95 s and1.38x10^{11}, 1.03x10^{11}, 7.90x10^{10}, 6.70x10^{10}, 5.89x10^{10} cm^{-2}, respectively.

ACKNOWLEGEMENTS

This project was financially supported by KMITL under grant No. 2555-A118-0220.

REFERENCES

[1] F. Gao, X.J. Liu, J.S. Zhang, M.Z. Song and N. Li: J. Appl. Phys. Vol. 111 (2012), pp. 084507-1-084507-3.

[2] H. Zhu, J. Zhang, C. Li, F. Pan, T. Wang and B, Huang: Thin Solid Films Vol. 517 (2009), pp. 5700-5704.

[3] F. Jaing, H. Shen, C. Gao, B. Liu, L. Lin and Z. Shen: Appl. Surf. Sci. Vol. 257 (2011), pp. 4901-4905.

[4] H.K. Yadav, V. Sreenivas and V. Gupta: App. Phys. Lett. Vol. 96 (2010), pp. 23507-1-2230507-3.

[5] N.R. Mathew, H.B.M. Anaya. M.A. Cortes-Jacome, C. Angeles-Chavez and J.A.Toledo-Antonio: J. Electrochem. Soc. Vol. 157 (2010), pp. H337-H341.

[6] B.C. Huang and Y.J. Lin: Appl. Phys. Lett. Vol. 99 (2011), pp. 113301-111303-3.

[7] Gu, M.G. Kanne, J.E. Doty and A .H. Firester: Appl. Phys. Lett. Vol. 87 (2005), pp.243512-1-243512-3.

[8] S.A. Studenikin, N. Gelego and M. Locivera: J. Appl. Phys. Vol. 83 (1998), pp 2104-2111.

6.2 ชื่อบทความวิจัยที่อยู่ระหว่างการดำเนินการ "Preparation of CuO Thin Films by Thermally Oxidized Metallic Cu Films for CdS/CuO Heterojunction Diode" ดังมีรายละเอียดดังนี้

ABSTRACT

Copper thin films were deposited on glass substrates using thermal evaporation in vacuum and then thermally oxidized in air at temperature ranging 100-500^{o}C. XRD patterns show the formation of fine grain Cu_2O phase at 300^{o}C and CuO phase at 400^{o}C, respectively. Crystallinity and grain size were found to improve with increasing oxidation temperature. The energy gap of the samples evaluated from absorption measurements was found to be in between 2.10 and 2.23 eV. Important electrical parameters such as resistivity, carrier concentration and mobility of CuO thin films obtained from oxidation temperature 500^{o}C are 8.53x10^{3} Ω·cm, 7.60x10^{13} cm^{-3} and 6.22 cm^{2}/V·s, respectively. The prototype of CdS/CuO thin film heterojunction diode was successfully prepared by thermal evaporation of CdS thin films on CuO thin films substrate in vacuum. The obtained device exhibits a good rectifying behavior from I-V characteristics. Various junction parameters such as barrier height, ideality factor and series resistance were calculated using I-V data and observed to be 5.190 eV, 0.520 and 3.87 Ω, respectively. Impedance spectroscopy of the device was investigated at temperature of 25-60^{o}C. The real and imaginary parts of the complex impedance are changed with the temperature and frequency. The experimental results suggest that the device could be possibly used a good candidate for photovoltaic devices with low thermal budget and low product cost.

Keywords: CuO thin films, thermal oxidation, CdS/CuO heterojunction, impedance spectroscopy

INTRODUCTION

Copper oxides are semiconducting materials that have a natural abundance of starting material Cu. They have been extensively studied because of their potential applications as solar cells, gas sensors, electrochemical sensors and batteries(Ooi et al. 2013; Valladares, 2012). Copper oxides are reported to be composed of two oxide phases, namely, cupric oxide (CuO) and cuprous oxide (Cu_2O) with p-type conductivity. The former has a narrow band gap of 1.21-1.51 eV absorbing throughout the visible spectrum with a monoclinic structure while the latter has a direct optical band gap range from 2.10-2.60 eV with a cubic structure (Cho et al., 2013). A meta-stable copper oxide, Cu_4O_3, which is an intermediate compound between the previous two, has also reported (Ooi et al., 2013). Numerous methods such as reactive sputtering, chemical vapor deposition, sol-gel, electro-deposition and thermal oxidation have been used to grow copper oxide thin films. In this work, we investigated the effect of

temperature of oxidation on the properties of copper oxide thin films prepared by oxidation of thermal vacuum evaporated Cu thin films. Structural, optical and electrical properties of the films were studied in order to find the possibility to use them in p-n junction. The formation of CdS/CuO heterojunction was elaborated by thermal evaporating CdS thin films on CuO thin films coated on ITO glass substrate. We investigated I-V and C-V characteristics of CdS/CuO heterojunction for evaluating some important parameters such as junction barrier height, ideality factor and series resistance values by using thermionic emission theory and Cheung's method. Moreover, impedance spectroscopy of the device was investigated at temperature range 25-60^{o}C.

MATERIAL AND METHODS

Copper thin films were grown on glass substrates by thermal evaporation in vacuum better than $5x10^{-5}$ mbar. Prior to deposition, the glass substrates were cleaned in acetone, ethanol and de-ionized water, respectively. The starting material was metallic Cu pellets (99.99% purity). The film thickness about 200 nm was monitored by a quartz crystal thickness monitor (Edward type FTM 6). The thermal oxidation of Cu films was carried out in a muffle furnace at difference temperatures ranging 100-500^{o}C for 60 min. The heating rate was maintained at 100^{o}C/h. After oxidation, the samples were cooled down to room temperature naturally. The crystal structure of these films was checked by X-ray diffraction technique with a Brucker D 8 diffractometer using CuK_{α} radiation. Surface morphology was examined by JEOL model JSM-6400 scanning electron microscope. Optical absorption measurements were performed with UV-VIS double beam spectrophotometer in the wavelength range of 220-800 nm. The band gap (E_g) of the transparent films was determined by using the equation $(\alpha h\nu)^2 = A'(h\nu - E_g)$ where α is the absorption coefficient, A' is a constant and $h\nu$ is the photon energy. Electrical properties of the films were evaluated by Hall effect and resistivity measurements in the van der Pauw configuration at room temperature. In order to fabricate CdS/CuO thin film heterojunction, Cu thin films deposited on ITO coated glass substrate and oxidized at 500^{o}C for 60 min. CdS thin films were subsequently evaporated onto CuO films. Finally, ohmic contact was made of silver paste on the surface of CdS and on the surface of ITO. The I-V characteristic curves were measured by using a computer interfaced Keithley 236 current/voltage source at room temperature. Impedance spectroscopy was carried out by Agilent E4980A Precision LCR Meter with frequency range 10 kHz- 2 MHz and temperature range 25-60^{o}C.

RESULTS AND DISCUSSION

Cu-O films characteristics

The XRD patterns of the as-grown and thermally oxidized Cu films at different temperatures ranging 100-500°C were shown in Figure 1. The as-grown Cu sample reveals a diffraction peak at 2θ equal to 43.50° corresponding to (111) diffraction plane of metallic Cu. Oxidation of Cu thin films at 100 and 200°C still shows purely (111) diffraction plane of metallic Cu phase with reduction in peak intensity. For the sample Cu films oxidized at 300°C, there is a weak diffraction peak at 36.46° which corresponds to the (111) plane of Cu_2O in agreement with the literature reported (Valladares et al., 2012). However, oxidation temperature at 400°C the (-111) diffraction plane of monoclinic CuO phase was occurred. For the films oxidized at 500°C the well- resolved two diffraction peaks at 2θ of 35.40° and 38.35° were observed. These peaks correspond to diffraction of (-111) and (111) planes of standard JCPDS data of CuO (JCPDS No. 80-1268). Figure 2 shows the SEM micrograph of Cu films oxidized at 500°C. The surface of the as-deposited Cu films is mostly smooth and uniform, while the surface particle size and surface roughness increase with the increase of thermal oxidation temperature.

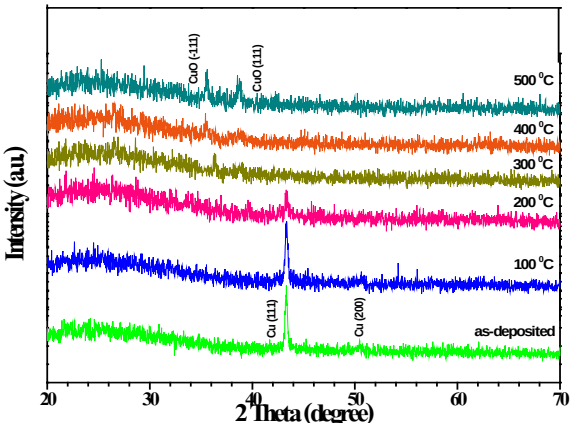

Figure 1. XRD patterns of Cu-O films.

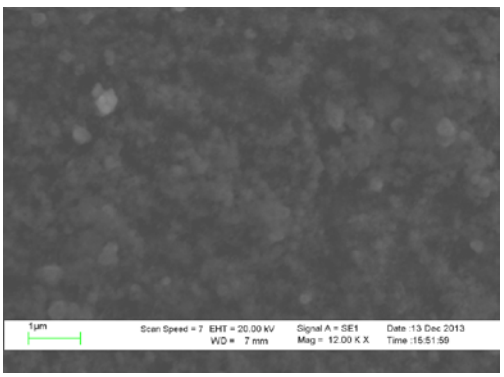

Figure 2. SEM micrograph of Cu-O films oxidized at 500°C.

Electrical properties of the films were evaluated by Hall effect and resistivity measurements in the van der Pauw configuration. We found that Cu films oxidized at 100-500°C are exhibited p-type conductivity. Variations of the resistivity(ρ), carrier concentration (p) and mobility(μ) against oxidation temperature are shown in Figure 3. Resistivity value of the as-deposited and the Cu films oxidized at 100°C is very low (~10^{-4} Ω·cm). It suggests that the main phase of the films oxidized at 100°C is still metallic Cu which is good agreement with XRD results. In contrast, the films oxidized at temperature beyond 200°C show high resistivity in the order 10^{3} Ω·cm. The carrier concentration initially decreases with an increase in oxidation temperature up to 300°C and then increases with an increase in oxidation temperature. The mobility is gradually decreased from 31.28 to 6.22 $cm^2/V{\cdot}s$ when the oxidation temperature increases from 100 to 500°C.

Figure 4 shows the absorbance (A) as a function of wavelength for the films oxidized at different temperatures. As seen, the absorbance value decreases as the wavelength increases. The absorption coefficient (α) can be calculated by using the relation; $\alpha = 2.303A/d$, where A is the absorbance and d is the thickness of the sample. From optical absorbance measurements the $(\alpha h\nu)^2$ data was obtained and, following the method reported by Tauc, were plotted as a function of photon energy ($h\nu$) to estimated the energy gap (E_g). Figure 5 displays the plot for Tauc's method to calculate the energy gap of the films oxidized at 300 °C. Variation of energy gap as a function of oxidation temperature is shown in Figure 6. The E_g value initially increases up to the maximun value 2.23 eV at oxidation temperature 300°C and then decrease to the minimum value 2.10 eV at oxidation temperature 500°C.

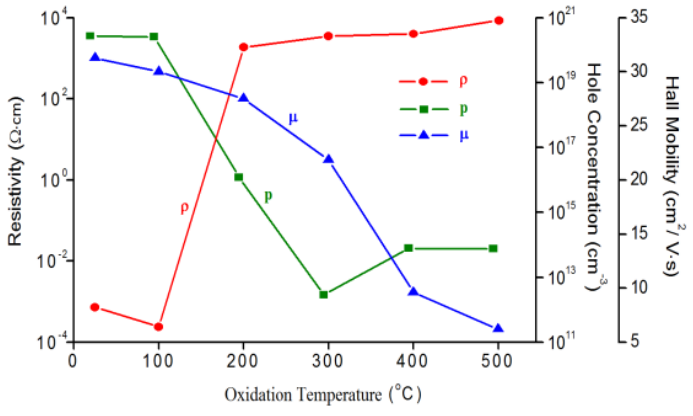

Figure 3. Variation of ρ, p and μ of Cu-O films.

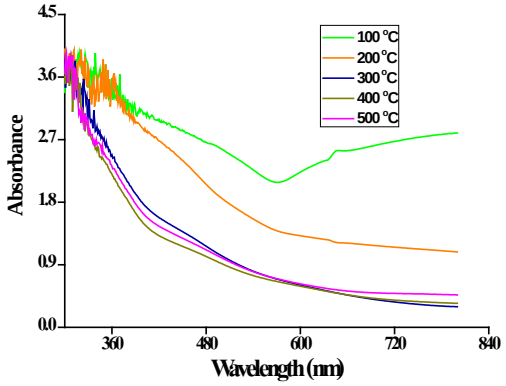

Figure 4. Absorption spectra of Cu-O films.

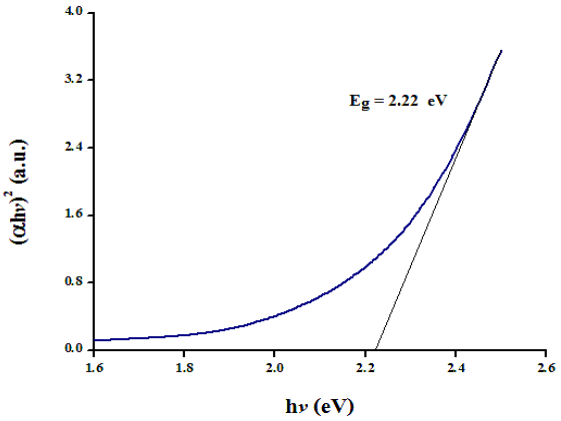

Figure 5. Plot of $(\alpha h\nu)^2$ vs. $h\nu$ of Cu-O films oxidized at 300°C.

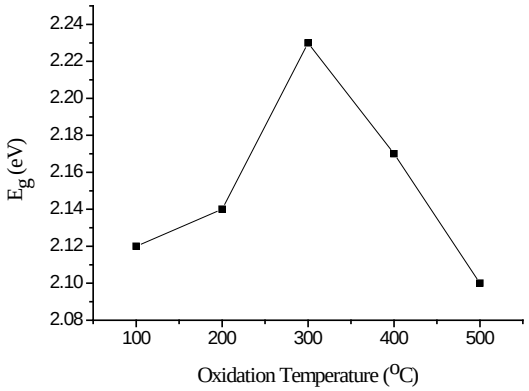

Figure 6. Variation of E_g with oxidation temperature.

Device characteristics

In the literature reviews, CdS compound has a higher resistivity than CuO and carrier concentration of CdS ($<10^{14}$ cm^{-3}) is lower than CuO ($>10^{16}$ cm^{-3}) about 3 order. Therefore, in the view of large different carrier concentration between CdS and CuO, it may be assumed that this heterojunction act as nearly a step junction. Therefore, it may assumed that the current through a diode

at a forward bias V, based on the thermionic emission (TE) mechanism, is given by the relation (Rhoderick and Willam, 1988)

$$I = I_s\left\{\exp(\frac{qV}{nkT})[1-\exp(-qV/kT)]\right\} \quad (1)$$

and

$$I_s = AA^*T^2\exp(-q\phi_{B0}/kT) \quad (2)$$

where I_S is the saturation current derived from the straight line intercept of the semi-logarithmic I-V plot at V=0, V is forward bias voltage, T is the absolute temperature, q is the electronic charge, k is Boltzmann constant, A is the effective area, $A^* = 4\pi qm_e k^2/h^3$ is the effective Richardson constant of 20 $A\cdot cm^{-2}\cdot K^{-2}$ for n-CdS, where $m^*=0.165m_0$ is the effective mass of the electrons, ϕ_{B0} is the apparent barrier height at zero bias voltage and n is the ideality factor. From Eq. (1), the ideality factor n which is given by

$$n = \left(\frac{q}{kT}\right)\left(\frac{dV}{d(\ln I)}\right) \quad (3)$$

The measured I-V plot of CdS/CuO diode at room temperature is shown in Figure 7. We have performed a least square fit of Eq. (1) to the linear part of the measured semi-logarithmic I-V plots (Figure 8) within bias voltage about 0.1-0.4 V. Once I_S is known, the zero bias barrier height (ϕ_{B0}) can also be computed with the help of Eq. (2). Using Eqs. (2) and (3), the experimental values of the ideality factor and the barrier height having 5.190 and 0.520 eV were determined. The observed high ideality factor suggests that the transport properties of the device could not be well defined by thermionic emission model. To better understand the mechanism that controls the transport properties of this heterojunction, lnI-lnV plot is presented in Figure 9. It is evident from lnI-lnV plot that forward bias characteristics show three regions. The first region (V<0.1V) I-V characteristics comply with the linear ohmic behavior (I~V), which is mainly caused by thermally generated charge carriers (Tyaki et al., 2015). In the region II ($0.1\leq V\leq 0.4V$) the current increases exponentially with bias voltage ($I \sim \exp\alpha V$). This is mainly to the recombination- tunneling mechanism (Aksoy and Cagar, 2012). At higher bias voltage (region III, V>0.4V) the I-V characteristics follow a power law relation ($I\sim V^2$). The current flow through the junction is due to space- charge limited current (SCLC) conduction, dominated by a single energy trap level (Zeyada et al., 2015). This SCLC mechanism is a normal phenomenon in the wide band gap semiconductor (Tyaki, 2015).

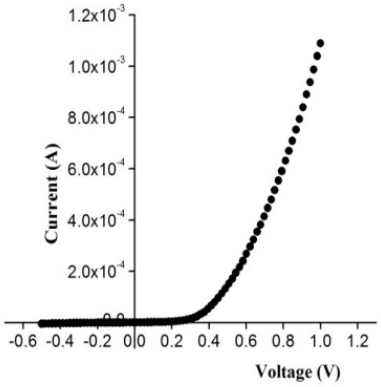

Figure 7. I-V plot of CdS/CuO diode.

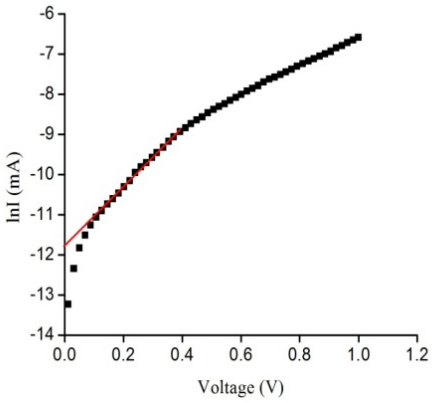

Figure 8. lnI-V plot of CdS/CuO diode.

The series resistance R_S is an important parameter in the electrical characteristics of diode. This parameter is significant in the downward curvature (non-linear region) of the forward bias I-V characteristics, but the other two parameters (n and ϕ_{B0}) are significant in both the linear and non-linear regions of the I-V characteristics. An efficient technique to determine R_S, n and ϕ_{B0} has been proposed by Cheung (Aksoy and Cagar, 2014). From Eq. (1) the following functions can be written as

$$\frac{dV}{d(\ln I)} = \frac{nkT}{q} + IR_s \tag{4}$$

$$H(I) = V - n\left(\frac{kT}{q}\right)\ln\left(\frac{I}{AA^*T^2}\right) \tag{5}$$

and H(I) is given as follows;

$$H(I) = n\phi_{B0} + IR_s \tag{6}$$

where ϕ_{B0} is the barrier height obtained from data of downward curvature region in the forward bias I-V characteristics. Eq. (4) should give a straight line for the data of downward curvature region in the forward bias I-V characteristics. Thus, a plot of dV/d(lnI)-I will give R_S as the slope and nkT/q as the y-axis intercept as shown in Figure 10. The values of n and R_s have been calculated as 5.322 and 3.48 Ω, respectively. This n value is slightly different obtaining from the forward bias lnI-V plot. This difference may be caused by the presence of series resistance and interface states (Barsoukov and Macdonald, 2005). Using the n value determined from Eq. (4) and the data of the downward curvature region in the forward bias I-V characteristics in Eq. (5), a plot of H(I)-I will also lead to a straight line with the y-axis intercept equal to $n\phi_{B0.}$ The slope of this plot also determines R_S, which can used to check the consistency of this approach. From the Figure 11, the barrier height and series resistance of the device are calculated as 0.542 and 3.87 Ω, respectively. Furthermore, the values of R_S obtained from dV/d(lnI)-I and H(I)-I plots are in good agreement with each other. This case shows the consistency of Cheung's approach.

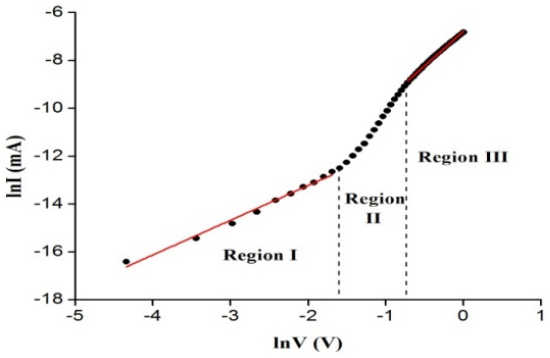

Figure 9. lnI-lnV plot of CdS/CuO diode.

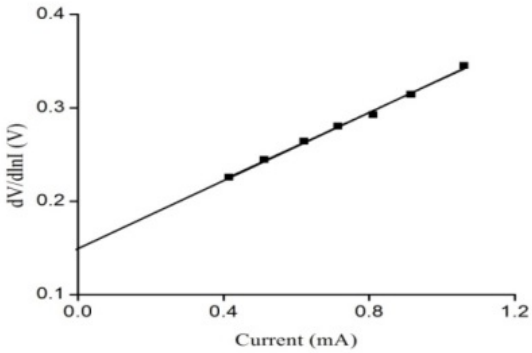

Figure 10. dV/d(lnI)-I plot of CdS/CuO diode.

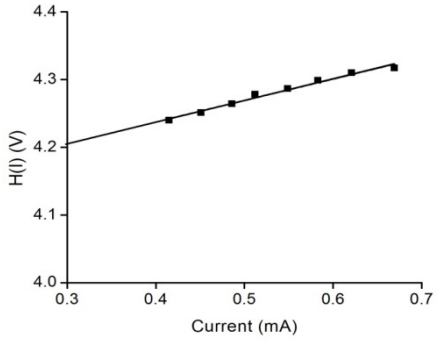

Figure 11. H(I)-I plot of CdS/CuO diode.

Figure 12 shows the variation of the real part of complex impedance (Z') with frequency at different temperatures. With increasing temperature, the curves display monotonous decrease in value of Z' with frequency. The magnitude of Z' decreases whereas temperature increases. It may indicate the increase in the a.c. conductivity. The Z' values merge above 100 kHz at all temperatures. Figure 13 shows the variation of the imaginary part of complex impedance (Z'') with frequency at different temperatures. The peak frequency of the Z'' shifts to higher frequencies with increasing temperature. This may indicate that decreasing relaxation in the system. The relaxation frequency (ω_0) was calculated from the peak frequency of Z'' plot with the help of the relation $2\pi f_0 RC=\omega_0 RC=1$[9]. This frequency was found to increase with temperature indicating increasing loss in the sample. From the Arrhenius plot of $\ln(\omega_0/T^2)$ as shown in Figure 14, the activation energy around 0.466 eV of the deep traps occurring at CdS/CuO interface was subsequently calculated. The appearance of discrete trapping level is in consistence with the results observed in d.c. transport studies corresponding to SCLC conduction controlled by single energy trap level.

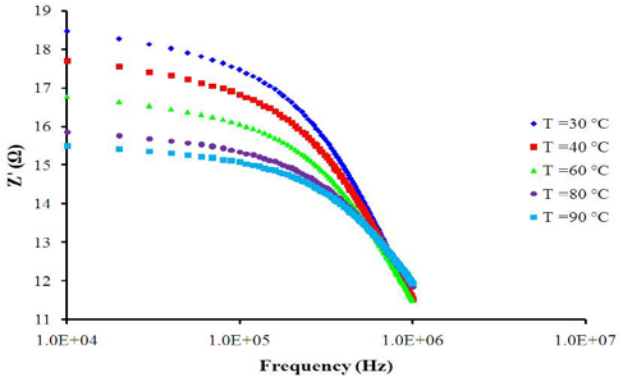

Figure12. Z'-f plot of CdS/CuO diode.

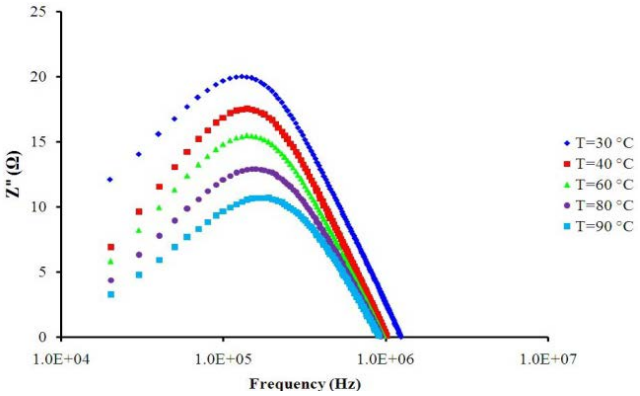

Figure 13. Z''-f plot of CdS/CuO diode.

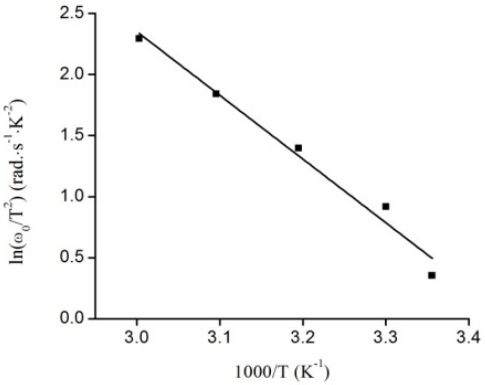

Figure 14. Arrhenius plot of $\ln\left(\omega_0/T^2\right)$.

CONCLUSION

Copper oxide thin films were successfully obtained through thermal oxidation process of Cu thin films, prepared by thermal evaporation in vacuum, at temperature beyond 200°C. From XRD patterns, a weak diffraction peak corresponding to (111) plane of Cu_2O phase was observed in the films oxidized at 300°C. For the films oxidized at 500°C, the well-resolved two diffraction peaks attributed to (-111) and (111) planes of CuO phase were appeared. From SEM micrographs, the surface particle size and surface roughness increase with the increase of thermal oxidation temperature. The dc electrical properties of the films were evaluated by Hall effect and resistivity measurements in the van der Pauw configuration at room temperature. The CdS/CuO heterojunction was successfully fabricated by thermal evaporation of CdS thin films on CuO thin films obtained by oxidation process at 500°C for 60min. The as-grown heterojunction shows a good rectifying behavior. The forward current transport is limited by three types of transport mechanisms namely Ohmic conduction, recombination-tunneling and space- charge limited current mechanisms depending on the applied forward bias voltage. Impedance spectroscopy of the device was investigated at temperature of 25-60°C. The real and

imaginary parts of the complex impedance are changed with the temperature and frequency. The experimental results suggest that the device could be used possibly a good candidate for photovoltaic devices with low thermal budget and low product cost.

ACKNOWLEDGMENTS

The authors would like to thank Assoc.Prof.Dr. T. Wongcharoen and Asst. Prof. Dr. C. Poo-Rakkiat for valuable discussions. This work was supported by King Mongkut's Institute of Technology Ladkrabang (grant number 2558A11802069/164817).

REFERENCES

Aksoy S. and Y. Cagar. 2012. Effect of ambient temperature on electrical properties of nanostructure n-ZnO/p-Si heterojunction diode. Superlattices and Microstructures 51: 613-625. DOI 10.1016/j.spmi.2012.02.018.

Aksoy, S. and Y. Cagar. 2014. Structural transformation of TiO_2 films with deposition temperature and electrical properties of nanostructure n-TiO_2/p-Si heterojunction diode. Journal of Alloys and Compounds 613: 330-337. DOI 10.1016/j.jallcom.2014.05.192.

Barsoukov E. and J.R. Macdonald. 2005. Impedance Spectroscopy: Theory, Experiment and Application, 2nd Edn., John Wiley & Sons, Inc., New York.

Cho, S. 2013. Optical and electrical properties of CuO thin films deposited at several growth temperatures by reactive rf magnetron sputtering. Metals and Materials International 19: 1327-1331. DOI 10.1007/s12540-013-6030-y.

Ooi, P.K., S.S. Ng, M.J. Abdullah, H. Abu Hassan and Z. Hassan. 2013. Effect of oxygen percentage on the growth of copper oxide thin films by reactive radio frequency sputtering. Materials Chemistry and Physics 140: 243-248. DOI 10.1016/j.matchemphys.2013.03.028.

Rhoderick, E.H. and R.H. William. 1988. Metal-Semiconductor Contacts. 2nd Edn., Oxford University Press.

Tyagi M., H. Toman and V. Gupta. 2015. Trap assisted space charge conduction in p-NiO/n-ZnO heterojunction diode. Material Research Bulletin 66:123-131.DOI 10.1016/j.materresbull. 2015.02.015.

Valladares L.L.S., D.H. Salinas, D.A. Najarro, S.I. Khondake, T. Mitrelias, C.H.W. Barnes, J.A. Aguiar and Y. Majima. 2012. Crystallization and electrical resistivity of Cu_2O and CuO obtained by thermal oxidation of Cu thin films on SiO_2/Si substrates. Thin Solid Films 520: 6368-6371. DOI 10.1016/j.tsf.2012.06.043.

Zeyada H.M., M.M. El-Nahass, E.M. El-Menyawy and A.S. El-Sawah. 2015. Electrical and photovoltaic characteristics of indium phthaloyanine chloride/p-Si solar cell. Synthetic Metals 207: 46-53. DOI 10.1016/j.synthmet.2015.06.008.